Reprint 2018-8

New data for representing irrigated agriculture in economy-wide models

K. Ledvina, N. Winchester, K. Strzepek and J.M. Reilly

Reprinted with permission from *Journal of Global Economic Analysis*, 3(1): 122–155.

The **MIT Joint Program on the Science and Policy of Global Change** combines cutting-edge scientific research with independent policy analysis to provide a solid foundation for the public and private decisions needed to mitigate and adapt to unavoidable global environmental changes. Being data-driven, the Joint Program uses extensive Earth system and economic data and models to produce quantitative analysis and predictions of the risks of climate change and the challenges of limiting human influence on the environment—essential knowledge for the international dialogue toward a global response to climate change.

To this end, the Joint Program brings together an interdisciplinary group from two established MIT research centers: the **Center for Global Change Science (CGCS)** and the **Center for Energy and Environmental Policy Research (CEEPR)**. These two centers—along with collaborators from the Marine Biology Laboratory (MBL) at Woods Hole and short- and long-term visitors—provide the united vision needed to solve global challenges.

At the heart of much of the program's work lies MIT's Integrated Global System Model. Through this integrated model, the program seeks to discover new interactions among natural and human climate system components; objectively assess uncertainty in economic and climate projections; critically and quantitatively analyze environmental management and policy proposals; understand complex connections among the many forces that will shape our future; and improve methods to model, monitor and verify greenhouse gas emissions and climatic impacts.

This reprint is intended to communicate research results and improve public understanding of global environment and energy challenges, thereby contributing to informed debate about climate change and the economic and social implications of policy alternatives.

—Ronald G. Prinn and John M. Reilly,
Joint Program Co-Directors

MIT Joint Program on the Science and Policy of Global Change

Massachusetts Institute of Technology
77 Massachusetts Ave., E19-411
Cambridge MA 02139-4307 (USA)

T (617) 253-7492 F (617) 253-9845
globalchange@mit.edu
http://globalchange.mit.edu

Journal of Global Economic Analysis, Volume 3 (2018), No. 1, pp. 122-155.

New Data for Representing Irrigated Agriculture in Economy-Wide Models

KIRBY LEDVINA[A], NIVEN WINCHESTER[B], KENNETH STRZEPEK[C], AND JOHN M. REILLY[D]

We develop a framework to represent the production value and expansion potential of irrigated land within economy-wide models, providing integrated assessment capabilities for energy-land-water interactions. The scope to expand irrigated land is quantified through irrigable land supply curves for 126 water regions globally based on water availability and the annual costs of irrigation infrastructure. Upgrades in irrigation infrastructure include (1) increasing water storage, (2) improving conveyance efficiency, and (3) improving irrigation efficiency. The value of production on irrigated and rainfed cropland is computed at both a 5 arcminute by 5 arcminute level and for the 140 regions and eight crop sectors in Version 9 of the Global Trade Analysis Project (GTAP) Data Base using estimates of production quantities and prices from the year 2000. This work facilitates the representation of endogenous investment in irrigation infrastructure and allows for a more rigorous exploration of the regional and global impacts of water availability on land use, energy production, and economic activity.

JEL codes: Q11, Q15, Q25

Keywords: Crop production; Disaggregation; Irrigation; Land supply; Water

1. Introduction

An expanding world population and global economy is expected to increase food demand and place pressure on current food crop production (Reilly et al., 2012; Wallace, 2000). Additionally, amidst a changing climate, new energy and climate policies may be proposed to support bioenergy production as an

[a] Joint Program on the Science and Policy of Global Change, Massachusetts Institute of Technology, 77 Massachusetts Ave, Cambridge, MA 02139 (kledvina@mit.edu). Corresponding author.
[b] Joint Program on the Science and Policy of Global Change, Massachusetts Institute of Technology, 77 Massachusetts Ave, Cambridge, MA 02139 (niven@mit.edu).
[c] Joint Program on the Science and Policy of Global Change, Massachusetts Institute of Technology, 77 Massachusetts Ave, Cambridge, MA 02139 (strzepek@mit.edu).
[d] Joint Program on the Science and Policy of Global Change, Massachusetts Institute of Technology, 77 Massachusetts Ave, Cambridge, MA 02139 (jreilly@mit.edu).

alternative to conventional fossil-based methods, placing food and energy production in direct competition for land resources (Calvin et al., 2014; Gillingham et al., 2008; Johansson and Azar, 2007; Popp et al., 2014; Smyth et al., 2010; Timilsina et al., 2012; Winchester and Reilly, 2015; Wise et al., 2014). One way to accommodate a growing demand for both food and bioenergy is to intensify existing crop land by increasing crop yields through investments in irrigation technology (Beringer et al., 2011; Taheripour et al., 2016). However, to explore the potential impacts of intensification on food prices and bioenergy production, we need to understand the physical and cost constraints on irrigable land expansion. How much additional land can be irrigated, in which parts of the world, and at what cost? While we can use applied general equilibrium (AGE) modeling techniques to investigate these questions, we first need the ability to explicitly represent irrigated land and its expansion potential within economy-wide models, a capability that is the main focus of this paper.

Early literature on separately representing irrigated and rainfed agriculture includes Taheripour et al. (2013a), Taheripour et al. (2013b), Liu et al. (2014), and Liu et al. (2016). However, the expansion potential of irrigated agricultural production has yet to be considered in the AGE literature. Thus, we advance current modeling practices by enabling the endogenous expansion of irrigated land through water region-specific irrigable land supply curves, which quantify the amount of irrigated land gained from investments in irrigation systems and water storage. The development of irrigable land supply curves to incorporate these responses within AGE models provides a mechanism for regions to expand production on irrigated land — subject to water constraints, infrastructure costs, and the availability of previously rainfed land. This capability allows for more robust exploration of the effects of a carbon policy and water constraints on economic performance, biomass production, land use, and greenhouse gas emissions.

We also extend earlier efforts to explicitly represent irrigated agriculture in the base year data of AGE models. Previously, Haqiqi et al. (2016) enhanced the Global Trade Analysis Project (GTAP) Power Data Base (Peters, 2016) — an augmentation of Version 9 of the GTAP Data Base (Aguiar et al., 2016) that represents electricity generation in detail — to separately represent rainfed and irrigated agricultural production and form the GTAP-Water Data Base. To disaggregate crop production value into rainfed and irrigated components, they use rainfed and irrigated output shares. This approach employs the simplifying assumption that irrigated land's share of total output quantity (in tonnes, t) is equal to its share of total output value (in U.S. dollars, USD) for each GTAP crop category. While this assumption seems reasonable for GTAP crop categories that consist of a single crop, it may not be valid for crop categories that include heterogeneous crops. Specifically, for heterogeneous crop categories, the production shares on irrigated and rainfed land may differ from output value shares if high-value crops are

grown on irrigated land and low-value crops on rainfed land, or *vice versa*. Though Haqiqi et al. (2016) note this possible issue, they do not explore the specific crops and regions for which differences may arise.

Thus, in addition to quantifying the expansion potential of irrigated agriculture, we also build on Haqiqi et al.'s (2016) work to represent base year irrigated agricultural production by using irrigated and rainfed value shares calculated with a global price dataset rather than output shares. While the output shares used by Haqiqi et al. (2016) are more attainable on a global scale, value shares bypass the implicit assumption that in each GTAP crop category the proportional cultivation of constituent crops on irrigated land is equal to that on rainfed land.

Altogether, the purpose of this paper is to elucidate and advance the development of this irrigated land framework. Specifically, we (1) provide estimates of the scope to increase irrigated land at the water region level and (2) assist the representation of irrigated land in the GTAP Data Base by improving estimates of production values shares on rainfed and irrigated land. Both items are tools that the modeling community may find useful, and we make our complete work stream available as supplementary materials. Specific materials include data on (1) irrigable land supply functions for 126 water regions, (2) irrigated and rainfed land area by GTAP region and crop sector, (3) the directly calculated value of irrigated and rainfed production by GTAP region and crop sector, and (4) source code for all aggregation routines.[1] The supplementary files allow aggregation of rainfed and irrigated land area, output volume, and production value from a finer level of spatial resolution to user-defined regions other than the GTAP regions. We also analyze the approach of Haqiqi et al. (2016) and flag regions and crop sectors where it may not be suitable to equate production shares with value shares.

The remainder of this paper describes the irrigated land framework and tools used. Section 2 details the construction of irrigable land supply curves. Section 3 discusses the valuation of irrigated and rainfed crop production. Section 4 summarizes the code and other tools we make available. Section 5 concludes.

2. Representation of Irrigable Land Supply Curves

The development of irrigable land supply curves enables regions to adapt to changes in water resources and agriculture demand by investing in irrigation infrastructure and intensifying crop production. To account for variations in water resources across river basins, we use 282 river basins defined by the Integrated Global Assessment Model – Water Resource System (IGSM-WRS) framework (Strzepek et al., 2013). Because river basins are in part delineated by political

[1] Haqiqi et al. (2016) also provide irrigated and rainfed crop areas by GTAP region and crop, as well as the GAMS code to generate irrigated and rainfed production values calculated from output shares.

borders, we define 126 water regions as aggregations of adjacent river basins that can cross country lines to better capture the transnational aspect of water resource systems. **Figure 1** maps the river basins and their water region aggregations.

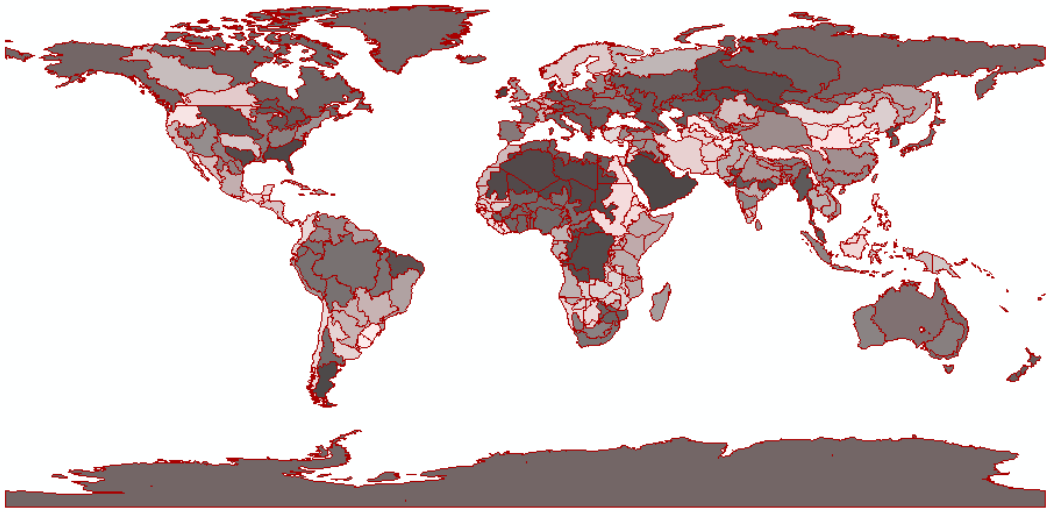

Figure 1. River basins (outlined) and their water region aggregations (shaded).

Notes: Shapefile is provided in the 1_SpatialData\SHP subfolder of the supplementary materials.

Source: Regional definitions as used by Strzepek et al. (2013)

2.1 Irrigation efficiency

We use irrigation system efficiency (SEF) values from the International Food Policy Research Institute's (IFPRI) International Model for Policy Analysis of Agricultural Commodities and Trade (IMPACT) model (Rosegrant et al., 2012) to characterize the current extent of irrigation in each of the 282 river basins. The SEFs of the 126 water regions are the average of constituent basin efficiencies, weighted by the area of irrigated land. Basin irrigation efficiencies in the base year 2000 are calculated as crop consumptive use divided by water delivered to irrigated land within the basin. Based on Food and Agricultural Organization (FAO) irrigation and drainage data (FAO, 2015b) and expert knowledge, we split the water region SEF values into two separate efficiency metrics for the base year: conveyance efficiency and field efficiency. The conveyance efficiency is determined by the amount of water lost to seepage and/or evaporation within a system of canals. Field efficiency — referring to the portion of the water released on the fields that ultimately waters the crops — depends on the type of irrigation system and increases with more targeted methods.

To allow for irrigation upgrades, we consider improvements in conveyance efficiency through the addition of canal lining. As most major irrigation canals are currently unlined, we assume all water region systems are initially unlined with a 75% conveyance efficiency (i.e. 75% of water released from dams reaches the field),

which increases to 95% with the addition of plastic or concrete lining. These approximations are assumed to apply to all water regions, following the approach in the IFPRI IMPACT model (Rosegrant et al., 2012). Each water region can also improve its field efficiency beyond its base year efficiency through four possible system upgrades at increasing annual costs: flood, furrow, low-efficiency sprinkler, and high-efficiency sprinkler. A representative irrigation technology currently in use is selected according to field efficiency in the base year, as summarized in **Table 1**. In each water region, additional investments in field irrigation systems can be used to improve field efficiency.[2] **Table 2** lists the efficiency values associated with each possible irrigation upgrade, as well as the new SEF incorporating the updated field efficiency. Because of the global scale of this work, we apply upgrade efficiencies to all river basins around the world. While these are indicative efficiency values (see FAO, 1989) combined with the authors' professional experience, field studies have also observed similar ranges (e.g. Fipps, 2000).

Table 1. Field efficiencies and corresponding irrigation technologies in base year 2000

Field Efficiency Range		**Corresponding Technology**
Low	***High***	
0	0.35	None
0.35	0.55	Flood
0.55	0.75	Furrow
0.75	0.85	Low-efficiency sprinkler
0.85	0.90	High-efficiency sprinkler

Source: Author-selected values

Table 2. Efficiency values from irrigation upgrades

Upgraded Field Technology	**(1) Field Efficiency**	**(2) Conveyance Efficiency**	**SEF (1)*(2)**
Flood	0.45	0.95	0.43
Furrow	0.65	0.95	0.62
Low-efficiency sprinkler	0.80	0.95	0.76
High-efficiency sprinkler	0.88	0.95	0.83

Notes: Field efficiency for each upgrade is the midpoint of the ranges from Table 1. Conveyance efficiency of 0.95 assumes lined canals.

Source: Author-selected values

[2] For rice paddy in the water regions, we allow only a one-time efficiency increase of 10 percentage points assuming good water management. There is growing literature on how to improve the water efficiency of paddy rice at the system level, but some technical issues remain difficult to model.

To determine the quantity of irrigated land gained with each system upgrade, we compute an updated sector water requirement (SWR) of irrigation, i.e. the water withdrawal required to meet irrigation demands of the current crop mix in each water region. A water region's SWR for irrigation is calculated as irrigated crop consumptive use across the water region divided by the region's SEF — this relationship highlights that because of transport inefficiencies, the amount of water allocated to irrigation exceeds the amount consumed by irrigated crops. Crop consumptive use is estimated for each water region using CliCrop (Fant et al., 2012) — a biophysical crop model that considers temperature, precipitation, and potential evapotranspiration — integrated with IGSM-WRS. We assume the crop mix remains constant over time — because of climatic similarity within the water regions, and considering that most irrigation is for cereals, there is a small range of per hectare water demand within each region. Altogether, we use the data on irrigation efficiency to calculate the water saved from an irrigation upgrade, and then, knowing the amount of water needed by the current crop mix, we determine how much additional land can be irrigated from the surplus water.

Of the possible improvements to conveyance and field efficiency, the addition of canal lining allows for the greatest increase in irrigable land at the lowest cost per hectare and is therefore the first irrigation system upgrade for all water regions, followed by upgrades in field technology in order of increasing field efficiency. Some irrigation upgrades in some water regions, typically high-efficiency sprinkler, are assumed to be infeasible because the resulting irrigated land expansion would exceed the quantity of available rainfed land.

Some water regions require manual adjustments to the estimates of additional hectares (ha) that can be irrigated. Specifically, the IGSM-WRS model overstates the amount of water saved from the addition of canal lining in large rice-producing water regions in China. This overestimation is a result of rice cultivation methods. Because rice paddies are grown in flooded fields, water that leaks out of unlined canals contributes to crop irrigation. Consequently, the addition of lining does not substantially improve irrigation efficiency, and the amount of additional irrigable land calculated from the IGSM-WRS output is overstated. We address this issue by setting the amount of additional land that can be irrigated due to the addition of canal lining equal to one-tenth of the estimated amount in eight water regions in China.[3]

2.2 Increases in water storage

Beyond improvements in irrigation efficiency, irrigable land in a water region can expand through investments in water storage. Each region's water storage capacity is modeled through a storage-yield curve relating available water supply

[3] These regions are SE_Asia_Coast, Chang_Jiang, Hail_He, Hual_He Langcang_Jiang, Songhua, Yili_He, and Zhu_Jiang water regions

to the quantity of storage. A region's storage-yield curve extends from no storage, which creates no additional irrigated land, to the amount needed to accommodate the region's mean annual runoff. Mean annual runoff is based on estimates of surface and subsurface runoff generated by the Community Land Model (CLM) (Bonan et al., 2002) within the IGSM framework (Sokolov et al., 2005). In modeling surface runoff, CLM considers the effect of soil infiltration limits, runoff from saturated surface conditions, frozen soil, and root density on soil hydraulic conductivity. Subsurface runoff is limited to the sustainable yield and is used by the Municipal, Industrial and Livestock sectors in that order of priority. Any surplus is added to the yield from the current reservoir storage, which is then available for irrigation. Additionally, for subsurface runoff CLM employs within each water region a representation of an unconfined aquifer, as opposed to the alternative artesian aquifer, which restricts water from entering through the top and bottom of the reservoir. The unconfined system is employed because it is less complex to model and because there is not yet academic consensus on the extent of each type of aquifer storage. Wiberg and Strzepek (2005) and Strzepek et al. (2013) further detail the storage capacity modeling and cost curve integration.

We divide each water region's storage-yield curve into ten possible upgrades of equal capacity but increasing marginal cost, with the assumption that lower cost upgrades are the first adopted. In each region, the storage-yield curve is combined with a storage-cost curve and an estimate of current storage to calculate the scope and cost of increasing annual water yields beyond the current storage level. Estimates of current storage in each region are sourced from the IMPACT model, which uses data from an online, global database of large dams managed by the International Commission on Large Dams (ICOLD). To determine the annual cost of additional storage, we source investment costs from FAO (2015b) and use IGSM-WRS, which takes water runoff data as an input, to determine both the marginal cost and the increase in yield volume from the capacity upgrade. We assume that additional storage upgrades are not adopted once capacity can fully accommodate the mean annual runoff. As with the irrigation system upgrades, we then consider the increase in water yield along with the current crop consumptive use and most updated irrigation efficiency values to estimate the quantity of irrigated land gained from the new storage upgrade.

2.3 Constructing supply curves for additional irrigated land

We arrange the five possible irrigation efficiency upgrades and ten possible storage upgrades into supply curves for additional irrigable land for each water region. The supply curves convey the number of additional hectares that could be irrigated and the annual cost per hectare of the infrastructure upgrades. Capital costs are annualized assuming a 50 year lifetime and a discount rate of 5%. Inputs of previously rainfed land are also required to expand irrigable land production. Increases in water available for irrigation — even from improvements in irrigation

efficiency — are used exclusively for the expansion of irrigated land. Therefore, the marginal product of both existing and newly irrigated land in each water region remains equal and constant as irrigated land expands within a water region.

As an example, the irrigable land supply function for the Mississippi River (MIS) water region is illustrated in **Figure 2** with corresponding data provided in **Table 3**. In this example, the additional irrigable land supply function includes seven incremental storage upgrades before maximum storage is reached, indicating that existing storage capacity is the sum of the first three incremental storage upgrades. As with all of the water regions, the addition of lining is the lowest cost efficiency upgrade, and because the next irrigation system upgrade is to a furrow system, it can be inferred that flood irrigation is used as the representative system for this water region. In total, investment in irrigation and storage infrastructure in the MIS water region could irrigate an additional 7.0 million ha beyond the current 3.0 million ha of irrigated land. Because the supply curves assemble additions to irrigable land from low to high investment cost, the supply curves represent the marginal cost of additional irrigable land.

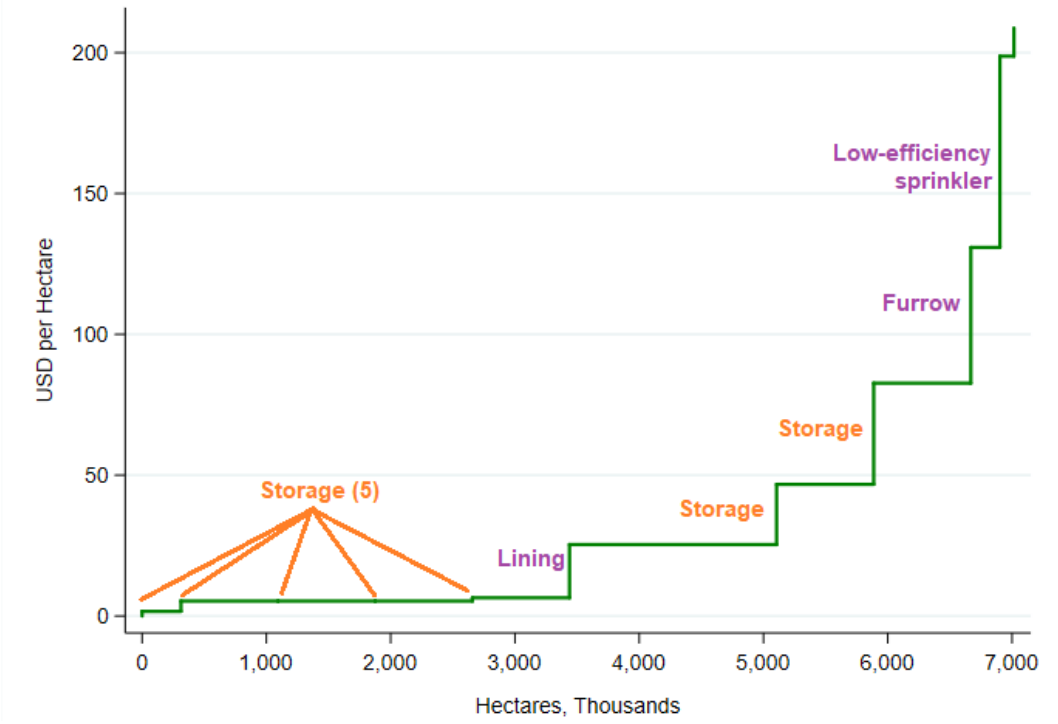

Figure 2. Irrigable land supply curve for Mississippi River (MIS) water region.

Source: Authors' calculations.

Table 3. Additional irrigable land from upgrades in Mississippi River (MIS) water region

Upgrade	**1**	**2**	**3**	**4**	**5**	**6**	**7**	**8**	**9**	**10**
Type	Stor.	Stor.	Stor.	Stor.	Stor.	Lining	Stor.	Stor.	Furrow	Low-eff. sprinkler
Yearly Cost (USD/ha)	1.62	5.30	5.30	5.30	6.46	25.36	46.73	82.67	130.85	198.75
New Irrig. Land from Upgrade (1,000 ha)	313	781	781	781	781	1,666	781	781	234	113
Total New Irrig. Land (1,000 ha)	313	1,095	1,876	2,658	3,439	5,106	5,887	6,669	6,902	7,015

Notes: Water supply limitations preclude investment beyond the tenth upgrade

Source: Authors' calculations.

Data on upgrade types, costs, and expansion possibilities for all water regions are provided as supplementary materials.[4] As a summary of these global datasets, **Figure 3** conveys the share of total potentially irrigable land that is currently irrigated in each water region while **Figure 4** illustrates each region's current marginal cost of irrigation infrastructure upgrades. Comparison of these two figures reveals that regions with greater irrigated land expansion potential, such as the Amazonian water regions, also generally face high technology costs and thus a deterrent to additional irrigation investment. However, some regions like the arid environments of North Africa and Southwest Asia have little irrigation expansion potential because of water resource limitations, though the annual costs are relatively low.

[4] See WaterRegionSupply.xlsx in the 3_SupplyCurves subfolder. A key to upgrade types is included in the Readme file.

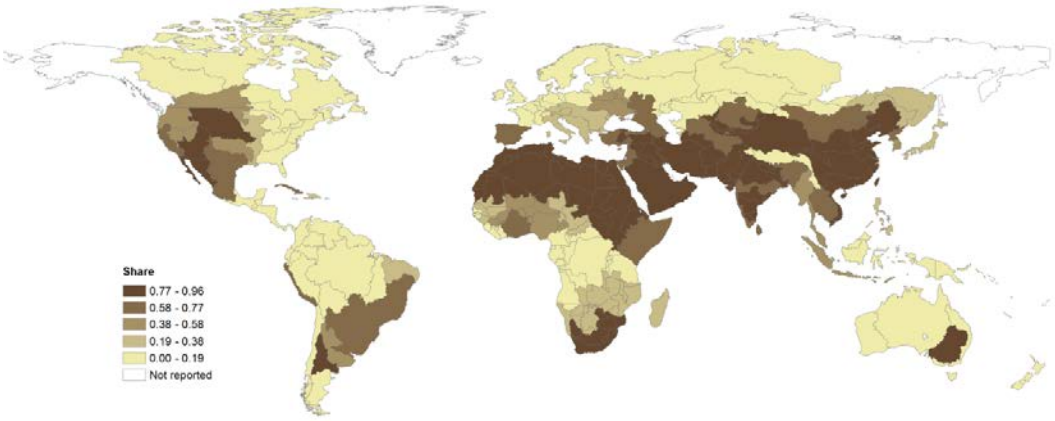

Figure 3. Irrigated agriculture's current harvested area as a fraction of total potentially irrigable land.

Notes: Data for the Rest of World water region (includes residual river basins in Alaska, Greenland, Iceland, Eastern Russia, Antarctica and North Korea) are not reported in the figure.

Source: Authors' calculations using Portmann et al. (2010)

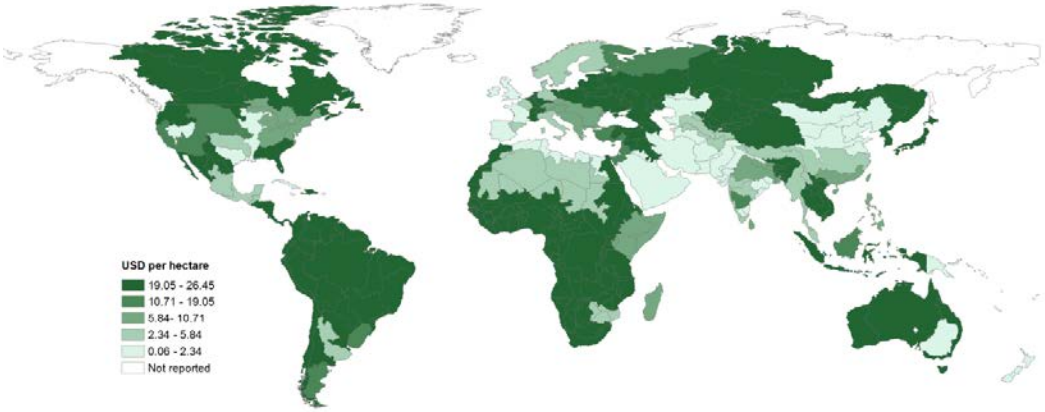

Figure 4. Current annual per-hectare cost of additional investments in irrigation infrastructure.

Notes: Data for the Rest of World water region (includes residual river basins in Alaska, Greenland, Iceland, Eastern Russia, Antarctica and North Korea) are not reported in the figure.

Source: Authors' calculations.

2.4 Including irrigable land supply curves in an economy-wide model

Winchester et al. (2018) include supply curves for additional irrigable land in the Economic Projection and Policy Analysis (EPPA) model, an economy-wide model that represents 16 global regions (Chen et al., 2017). For modeling tractability, they define irrigation response units (IRUs) as groups of water regions

with similar crop yields within an EPPA region. They determine IRU membership using a k-means cluster analysis of water regions based on their rainfed and irrigated yields. Each EPPA region contains between one and four IRUs, yielding 46 IRUs globally. The IRU assignments for all regions are summarized in **Table A.1** in **Appendix A**. The Stata code for the cluster analysis and a collection of figures illustrating the results in each region are included in the supplementary materials. [5] As an example, **Figure 5** depicts the cluster analysis results in the Latin America (LAM) region.

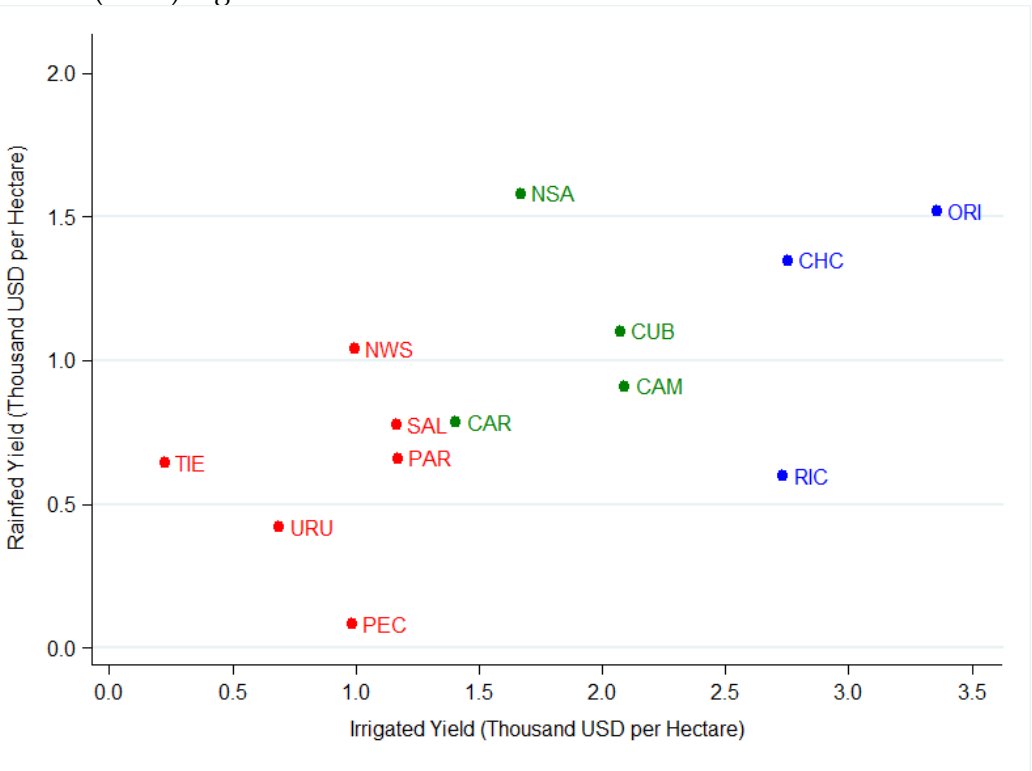

Figure 5. Cluster analysis of water regions to form irrigation response units (IRUs) within the Latin America (LAM) EPPA region.

Notes: IRUs are distinguished by color.

Source: Authors' calculations.

The irrigable land supply curves of constituent water regions are aggregated to form IRU supply curves for additional irrigable land. To approximate step irrigable land supply curves as 'smooth' functions, a supply elasticity parameter of the form $q = \beta p^{\lambda}$ is econometrically estimated to fit each IRU step function, with

[5] See ClusterAnalysis.do in the 3_SupplyCurves subfolder.

quantity in thousands of ha as q and price in USD per ha as p.[6] An exponential form is adopted so that the supply elasticity λ will remain constant for an IRU at all quantities of irrigated land. Supply curves for additional irrigable land can be modeled using constant elasticity of substitution functions following the procedure outlined by Rutherford (2002). In the base year in EPPA, each IRU's quantity of irrigated land is set proportional to its contribution to aggregate production value within the EPPA region, with total land endowment remaining fixed from 2005 to 2050, the timespan modeled. The method and data for quantifying the current scope of irrigated agricultural production is described in Section 3.

Using the IRU-level irrigable land supply elasticities, Winchester et al. (2018) augment the EPPA model to allow additional irrigated land to be produced by combining rainfed land with capital representing investment in irrigation infrastructure. In their model, crop land can be expanded by converting land from other agricultural uses and also the conversion of non-managed land to agricultural uses.

Calibrating the production functions for additional irrigable land requires, for each region, (1) annual rental costs per hectare of (previously) rainfed land, and (2) annual capital costs (representing payments to irrigation infrastructure) per additional hectare of irrigable land. Winchester et al. (2018) calculate land rental costs in each region by dividing total rental payments to crop land by the number of hectares in crop production estimated by Portmann et al. (2010). For the first additional hectare of irrigated land in each IRU, annual rental payments to irrigation infrastructure (capital) equal the annualized cost of the first (least-cost) irrigation upgrade option. Irrigation infrastructure costs rise as more hectares are irrigated according to the 'smooth' supply curves fitted to the step-supply functions (see Figure 2 for an example). As such, the cost share of irrigation infrastructure varies across regions and, within each region, increases as more hectares are irrigated.

Although Winchester et al. (2018) apply supply elasticities at the IRU level, irrigable land supply curves could be specified for each water region or for a user-defined aggregation of water regions for use in other AGE models. The irrigable land supply curves could also be applied in AGE models that do not have a detailed land-use change module, but alternative assumptions about the availability of crop land would result in different estimates of irrigation (and agricultural) outcomes.

[6] See SupplyCurves.gms for the script to aggregate and econometrically estimate IRU supply curves

3. Production on irrigated land and rainfed land

As AGE models are calibrated using transaction values, a key requirement in separately representing irrigated and rainfed crop production is the division of aggregate crop production into separate production values for irrigated land and rainfed land. As noted above, Haqiqi et al. (2016) have incorporated an irrigated land framework into the GTAP-Power Data Base to form the GTAP-Water Data Base. They estimate irrigated and rainfed production value by first identifying the volume of production on irrigated and rainfed land and splitting the aggregate value of production in a GTAP crop sector according to each land type's share of crop output. We extend the methodology used by Haqiqi et al. (2016) by applying crop and region specific prices to rainfed and irrigated crop production. To evaluate the substitutability of the two methods to estimate production value shares, we incorporate crop prices, and compare the resulting production values to estimates based on output shares. Within a region, production value shares generally equal the output shares for individual crop sectors (e.g. wheat) but can diverge for composite crop sectors (e.g. coarse grains), because of differences in individual crop prices and the mix of composite crops grown on the two land types. We make available rainfed and irrigated production values for 26 disaggregated crops at the 5 arcminute by 5 arcminute (about 0.083 square degrees, or 10 square km at the equator) grid cell level and for 282 river basins, as well as for the 140 GTAP regions and eight crop sectors considered in the GTAP-Water Data Base.

3.1 Direct calculation of production value

Following Haqiqi et al. (2016), we use spatial datasets on harvested areas and crop yields to calculate production volumes, which we combine with country-level data on crop prices to estimate crop production value on rainfed and irrigated land. We obtain harvested areas for rainfed and irrigated land from the Monthly Irrigated and Rainfed Crop Areas (MIRCA2000) dataset (Portmann et al., 2010). Areas are reported for the year 2000 and are available globally for 26 crops and two land types at a 5 arcminute by 5 arcminute spatial resolution.[7] **Figure 6** provides a snapshot of the grid cell-level MIRCA2000 dataset for barley with relative amounts of irrigated and rainfed crop areas overlaid on a map of GTAP 9 regions.

[7] The full spatial dataset of harvested areas is included in the 1_SpatialData subfolder of the supplementary materials.

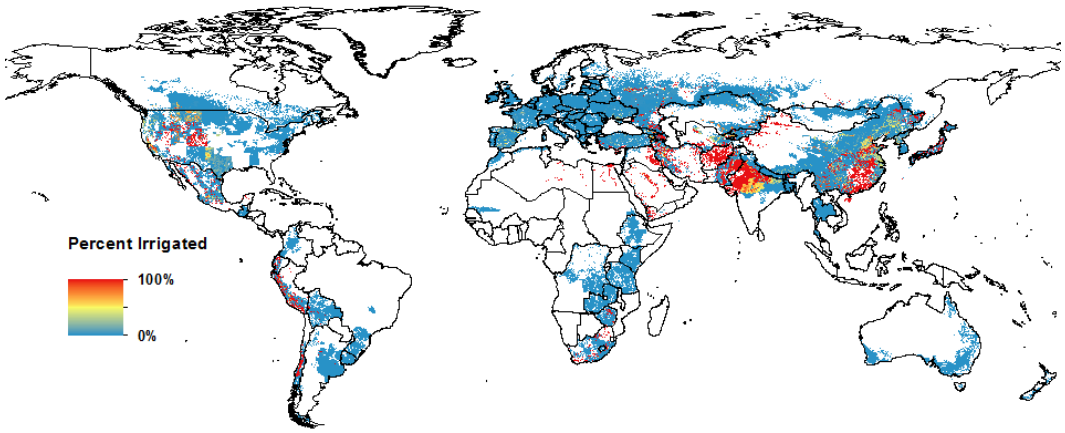

Figure 6. Percentage of harvested barley in each grid cell coming from irrigated production. White areas have no barley production.

Source: Authors' aggregation of Portmann et al. (2010).

The high resolution of the MIRCA2000 dataset allows for flexibility in how the harvested areas are aggregated, whether regionally or globally. Because the GTAP databases are ubiquitous in economic modeling, for illustration purposes, we calculate harvested area for the 140 regions and 8 crop sectors represented in the GTAP 9 Data Base. **Figure 7** summarizes the global harvested area of each GTAP crop by land type. Globally, seventy-six percent of cropland is rainfed, with paddy rice (pdr) the only crop primarily grown on irrigated land.

Data on rainfed and irrigated crop yields are sourced from Siebert and Döll (2010) and are available at a 5 arcminute by 5 arcminute spatial resolution for 29 crops.[8] These 29 crops include the original 26 crops covered by the MIRCA2000 dataset but with (1) three types of animal feed rather than a single fodder category, and (2) the addition of pasture land, which we exclude from our analysis. We take a simple average of 'fodder from maize', 'fodder from barley', and 'fodder from wheat' yields to approximate a single fodder yield at the grid cell level for each land type. Yields of 0 tonnes per hectare (t/ha) for a specific fodder crop are reclassified as missing data and excluded from the average for that particular grid cell. We calculate tonnes of production by land type and crop as the product of the harvested area and yield in each grid cell.

[8] The full spatial dataset of yields is included in the 1_SpatialData subfolder of the supplementary materials.

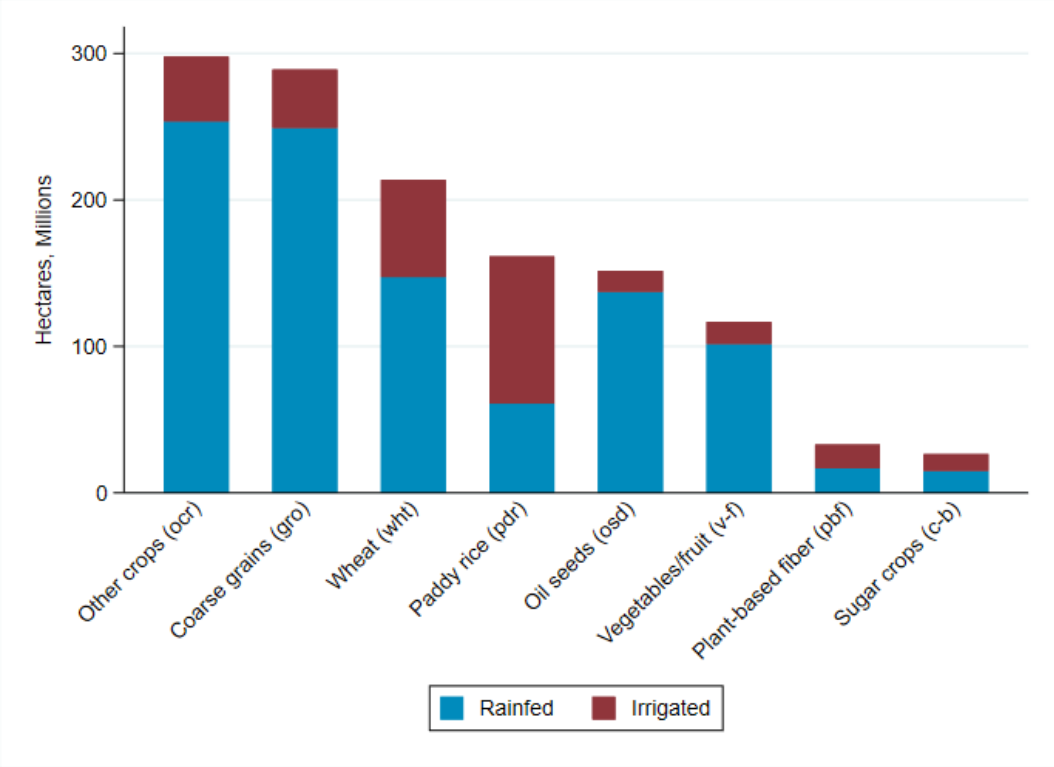

Figure 7. Global rainfed and irrigated harvested area by GTAP crop.

Source: Authors' aggregation of Portmann et al. (2010). Crop mapping from Haqiqi et al. (2016).

To determine the dollar value of rainfed and irrigated crop production, we apply crop prices obtained from an FAO dataset (FAO, 2015c) to the spatial production data. The FAO dataset consists of country-specific prices from the year 2000 for 215 crops and does not differentiate between crops grown on different land types.[9] In other words, crops grown on rainfed land and irrigated land within the same country are assumed to sell for the same price.

We create a raster dataset of prices that can be applied to production output at the grid cell level by (1) consolidating the 215 FAO crops into the 26 MIRCA2000 crop categories, (2) interpolating missing country-level price data, and then (3) pixelating the country-level data to create raster datasets.[10] We complete the first adjustment by assigning each FAO crop to one of the 26 MIRCA2000 crop categories and using FAO production data (FAO, 2015a) to compute a production-

[9] Price data is provided in FAOprices.xlsx in the 1_SpatialData\Prices subfolder of the supplementary materials.

[10] See the 1_SpatialData\Prices subfolder in the supplementary materials for the spatial price dataset. Instructions to update and regenerate the dataset are provided in the Readme file of the supplementary materials.

weighted price within each crop category.[11] The specific crop mapping employed is specified in **Table B.1** in **Appendix B**. We use a listing generated by the Natural Resources Conservation Service (NRCS) of the U.S. Department of Agriculture (USDA) to identify FAO crops classified as 'other annual' or 'other perennial' (NRCS, 2014).

We interpolate missing prices by separately handling (1) countries with no crop price data and (2) countries with some but not complete crop price data. The FAO provides no price information for 32 countries, so we substitute known prices from a geographically proximate country. **Table B.2** in **Appendix B** lists the pairings of countries missing price data and those selected to provide proxy prices. Country pairing assignments are determined on a geographic basis (e.g. Dominican Republic and Haiti, and Sudan and South Sudan). Although alternative assignments are unlikely to have a large impact at the aggregate level,[12] production values for countries with missing price data should be used with caution.

For cases where FAO (2015c) is missing prices for a subset of crops in a country, we estimate global prices of the missing 26 MIRCA2000 crops, with the understanding that several countries may have no production of the specific crop and will not affect aggregate value. We develop these missing country-level prices for each MIRCA2000 "target" crop (the crop missing price data) by using price ratios based on data from countries with known prices. Specifically, we use the ratio of the target crop's price to the price of several candidate "guide" crops — barley, citrus, maize, wheat, rice, potatoes, and groundnuts, or some combination of these crops — in a country with known prices for both the target and guide crops. The specific crop combination selected is based on the ratios with the lowest variance across countries.

For example, the FAO reports that Paraguay produced 82 thousand tonnes of sunflower seed in the year 2000, but FAO (2015c) does not report a producer price for this crop in 2000. To estimate the price of sunflower in Paraguay, for the countries with available price data, we compute a ratio of sunflower price to each guide crop's price and calculate the mean and variance for each ratio across countries. Because of their low variances, the groundnut, rice, maize, and potato ratios are used to generate four country-level sunflower price estimates,[13] which are averaged to produce a single price estimate. **Table 4** presents the ratio statistics for each guide crop and the calculations leading to a final sunflower price estimate for Paraguay of $249.10/t, which can be compared to $257.92/t, the simple average

[11] Production-weighted prices are calculated in Prices.gms in the 1_SpatialData\Prices subfolder of the supplementary materials.

[12] Countries with missing prices provide 3.6% of global crop output, according to FAO (2015a) data.

[13] For each country, an estimate is generated only if a price for the guide crop exists.

of known FAO sunflower prices across countries. An Excel workbook with this methodology and calculations for all crops and countries is included in the supplementary materials.[14]

Table 4. Sunflower Price Estimation in Paraguay

Guide Crop	(1) Mean of Country Ratios	(2) Variance of Country Ratios	(3) Price (USD per t) in Paraguay	Sunflower Price Estimate (USD per t) (1)×(3)
Groundnuts /peanuts	0.485	*0.036*	487.60	236.68
Rice	1.161	*0.265*	112.40	130.49
Maize	1.705	*0.310*	137.70	234.83
Potatoes	1.375	*0.485*	286.80	394.43
Citrus	1.338	*0.956*	104.37	139.64
Wheat	1.731	*1.134*	121.90	211.02
Barley	1.988	*1.226*	No Data	No Data
Averaged estimate (outlined cells only)				**249.10**

Source: Authors' calculations using FAO (2015c)

Finally, we generate a complete spatial dataset of prices for GTAP regions by (1) assigning each GTAP region an average price weighted by country area and then (2) pixelating the regional price data to form grid cell-level spatial data. We calculate production value at the grid cell level by multiplying output by crop prices.[15] For illustration purposes, **Figure 8** depicts our estimates of global production value by land type and crop when the estimates are aggregated to the eight GTAP crop sectors. Despite having approximately three times the harvested area as irrigated crops, rainfed crops generate only twice the value.

[14] See CropPriceInterpolation.xlsx in the 1_SpatialData\Prices subfolder of the supplementary materials.

[15] See GenerateRasters.py in the 1_SpatialData subfolder of the supplementary materials for the code to create the price, output, and value spatial datasets. See Aggregate.py in 2_ProductionValue for the code to aggregate the spatial data.

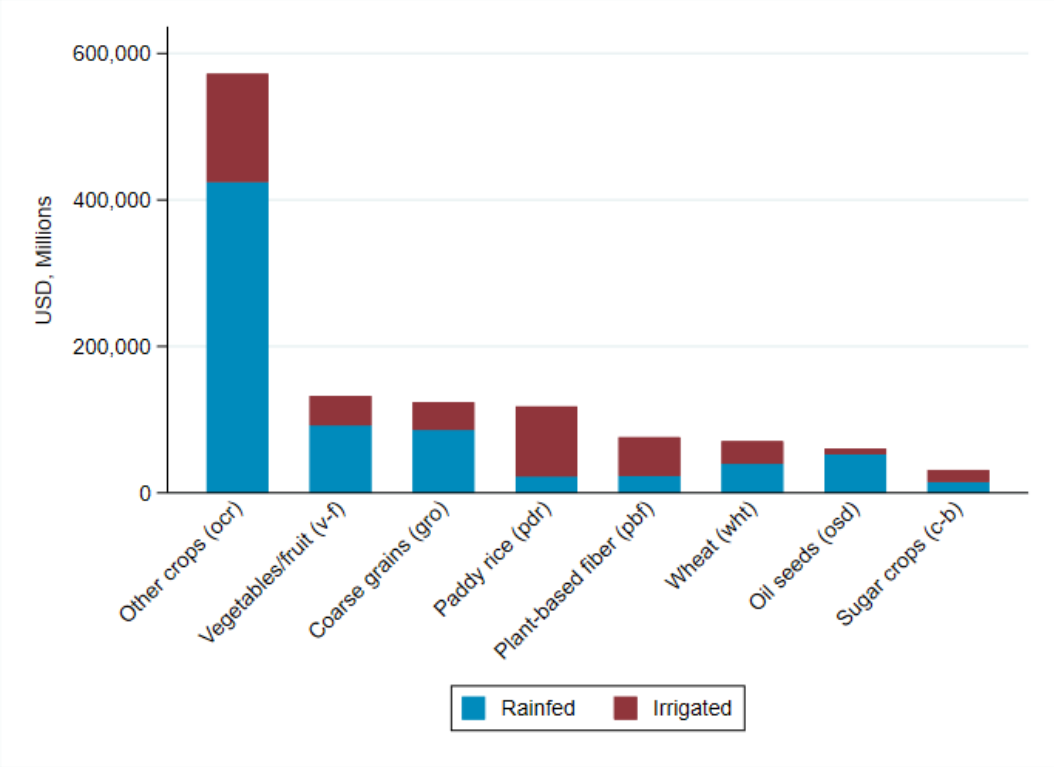

Figure 8. Global production value on rainfed and irrigated land by GTAP crop.

Source: Authors' calculation using Portmann et al. (2010), Siebert and Döll (2010), and FAO (2015a, 2015c). Crop mapping from Haqiqi et al. (2016).

Overall, our aim was to generate an initial version of a comprehensive production value dataset. The process we describe to determine production values at the five arcminute by five arcminute level maintains the spatially detailed harvested area and yield information provided by Portmann et al. (2010) and Siebert and Döll (2010). Additionally, the fine resolution provides flexibility for user-specified spatial aggregations of the data. Nevertheless, our method requires a high degree of price estimation in order to achieve global coverage, and we recognize the need for a more rigorous approach. For example, while we use a handful of crop prices from all countries to estimate missing data, future work could more thoroughly explore the correlation in prices of different subsets of crops and countries. Alternatively, where available, time series of crop prices could be used to estimate missing data for the year 2000 though we avoided this approach because of perceived fluctuations in FAO (2015c) price data. Looking forward, we welcome improvements to our first-step methodology, and the provided work stream and high resolution datasets should allow for updated local or county-level prices in future work.

3.2 Comparison of production methodologies

Using the estimates detailed in Section 3.1., we compare production value shares calculated (1) by multiplying output volumes by prices and (2) by assuming that production value shares are equal to output volume shares, as in Haqiqi et al. (2016). The goal of this comparison is to gain insight into where and for which crops the simplifying assumption used by Haqiqi et al. (2016) may or may not be valid. As further described in **Appendix C**, while results for the aggregate irrigated crop value are comparable under the two methods, estimates vary greatly when assessed by crop sector. This is because value shares approximated by output shares may not capture differences between production quantities and values within composite GTAP crop sectors, i.e. GTAP sectors containing multiple MIRCA2000 crops — oilseeds (osd), vegetables and fruit (v-f), coarse grains (gro), sugar crops (c-b), and other crops (ocr). However, three of the GTAP crop sectors — wheat (wht), paddy rice (pdr), and plant-based fiber (pfb) — consist of a single MIRCA2000 crop — wheat, rice, and cotton, respectively — and therefore should have identical estimates from output shares and from direct calculation of production values (prices do not differentiate between rainfed and irrigated crops). More generally, for a given crop in a particular region, the production value share on irrigated land will equal the corresponding output value share if (1) the production share of each MIRCA2000 crop within a composite GTAP sector on irrigated land is equal to that on rainfed land, as noted by Haqiqi et al. (2016); or/and (2) the prices per tonne for each MIRCA2000 crop within a composite GTAP sector are equal.

As illustrated in **Figure 9**, the vegetables and fruit sector (v-f) shows substantial regional variation in the value comparison. In the figure, the data point representing the United States, the largest irrigated v-f producer by both output and value, falls along the 45 degree line, indicating similar value estimates from the two calculation methods. In this region, the most produced v-f crops, citrus and potatoes, share a similar price — $108/t for citrus and $112/t for potatoes — while the third most produced crop, grapes/vines, has a higher price but contributes in similar proportions to USA irrigated and rainfed v-f production. In contrast, Thailand, which produces 90% of its v-f output on rainfed land, features a higher irrigated v-f value from direct calculation than from an output share estimation. This difference in value arises because rainfed cassava contributes to 88% of the Thailand's total v-f production but, with a price of $16/t, makes up just 22% of total value. In contrast, irrigated citrus contributes only 10% of the total v-f output in Thailand yet generates 66% of v-f value with its price of $419/t. Because highly cultivated rainfed crops generate less value than the irrigated crops, dividing total value into irrigated and rainfed parts based on output share may

not be a suitable method for the v-f sector in Thailand. Further analysis of other crop sectors is provided in Appendix C. [16]

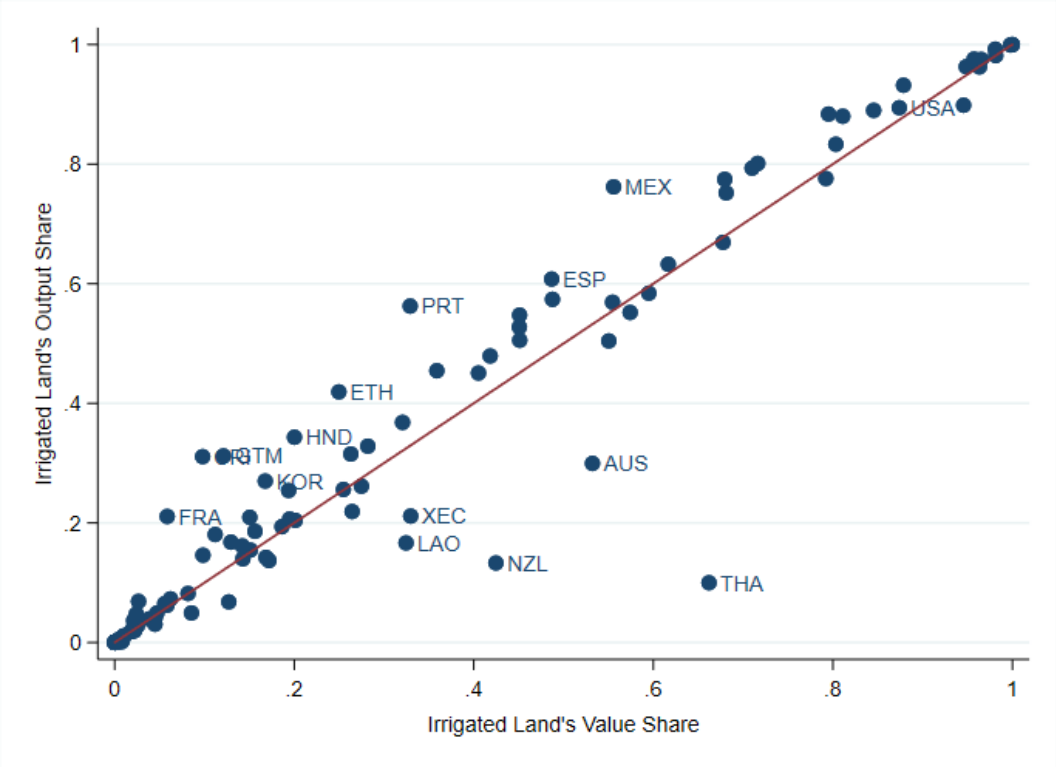

Figure 9. Irrigated share of production value estimated from the output share (y-axis) versus direct calculation (x-axis) for the v-f GTAP sector.

Notes: Points represent GTAP regions. The red line marks 45 degrees.

Source: Authors' calculation using Portmann et al. (2010), Siebert and Döll (2010), and FAO (2015a, 2015c). Crop mapping from Haqiqi et al. (2016).

To more formally evaluate the appropriateness of using output shares to approximate value shares, we calculate a relative error metric, $k_{c,r}$, for each GTAP crop category, c, and region, r, given by

$$k_{c,r} = \frac{p_{c,r} - v_{c,r}}{0.5 * (p_{c,r} + v_{c,r})} \quad (1)$$

where $p_{c,r}$ and $v_{c,r}$ are, respectively, the production value computed from output share and from direct calculation for crop c on irrigated land in region r. Relative error values for all GTAP crop-region combinations are provided in the

[16] Supporting data with output value shares and production value shares for each GTAP crop-region combination are provided in ValueSummary.xlsx in 2_ProductionValue subfolder of the supplementary materials.

supplementary materials included with this paper.[17] To focus on crop-region combinations where the assumption that the production share equals the value shares is most likely to be violated, **Table 5** lists the region-crop combinations with the highest absolute relative errors. Across all region-crop combinations, relative error values range from -1.48 (v-f in Thailand) to 1.13 (v-f in France) and yield an average absolute relative error of 0.12. Of the region-crop combinations with a non-zero relative error, fifty-four percent have a positive relative error, suggesting that use of the production share simplification tends to overestimate the value of production on irrigated land. For crop-country combinations with high absolute relative errors, we encourage the use of the tools and data detailed in this paper to adjust the irrigated land-augmented version of the GTAP-Water Data Base provided by Haqiqi et al. (2016).

Table 5. Largest 10 Irrigated Relative Errors

Region	Crop	Value share	Absolute relative error
Thailand (THA)	v-f	14.7%	1.48
Mozambique (MOZ)	v-f	28.7%	1.44
Indonesia (IDN)	v-f	7.4%	1.42
Indonesia (IDN)	osd	13.5%	1.33
Thailand (THA)	osd	3.0%	1.31
Azerbaijan (AZE)	osd	0.3%	1.24
France (FRA)	v-f	27.7%	1.13
United Kingdom (GBR)	ocr	69.0%	1.13
Taiwan (TWN)	ocr	71.0%	1.12
Malaysia (MYS)	v-f	0.6%	1.09

Notes: Value share refers to the crop sector's share of the region's total crop value.

Source: Authors' calculations.

4. Supplementary Materials

We provide our datasets and code to allow other researchers to replicate and build upon the production value analysis and supply curve construction. We hope these resources will support future work to improve the representation of agricultural productivity in AGE models, whether at a national or global level. **Table 6** summarizes the available supplementary materials.

[17] See ValueSummary.xlsx in the 2_ProductionValue subfolder. Related calculations are in GTAPreporting.gms.

Table 6. Important supplementary resources

Folder	Contents	File Name
1_SpatialData	Spatial data for crop areas, yields, output prices, and production value	
	Shapefiles for aggregation to water regions, countries, or GTAP regions	
	Code **(A)** and datasets (including **B**) to calculate prices for MIRCA2000 crops	**A. Prices.gms** **B. Prices\CropPrice Interpolation.xlsx**
	Code to regenerate price, output, and value spatial data	**GenerateRasters.py**
2_ProductionValue	Code to aggregate area, output, and value spatial data to desired regions (**A**) and resulting summary files **(B)**	**A. Aggregate.py** **B. Compiledarea_GTAP.csv, etc.**
	Code to create alternative value estimates by GTAP region and crop	**GTAPreporting.gms**
	Summary file with production values and evaluation metrics by GTAP region and crop	**ValueSummary.xlsx**
	Summary file with disaggregated crop prices and production shares by MIRCA2000 crop and GTAP region	**CropDisaggregation.xlsx**
3_SupplyCurves	Data for water region supply step functions	**WaterRegionSupply.xlsx**
	Code to perform water region cluster analysis	**ClusterData.gms**, **ClusterAnalysis.do**
	Scatterplots illustrating current cluster results	**Graphs**
	Code to create IRU irrigable land supply curves	**SupplyCurves.gms**

Source: Authors' compilation

5. Conclusion

The explicit representation of irrigated land within integrated assessment and economy-wide models can provide insights into how regions will balance growing demand for land amidst the changing availability of regional water resources, and is an important step for looking at energy-water-land interactions. To develop this irrigated land framework, modelers need to identify the current scope of irrigated land and define its potential for expansion. Previously, Haqiqi et al. (2016) formed the GTAP-Water Data Base to separate irrigated and rainfed land within an economy-wide model. However, to divide the production value for each crop into irrigated and rainfed components, they use estimates based on production volumes rather than a direct calculation of production values. While this approach is sufficient for some GTAP regions and crop sectors, irrigated production value shares based on output volumes differ from the directly calculated values in composite GTAP crop sectors within several regions because the mix of crops grown on each land type differs. Additionally, existing AGE analyses do not consider endogenous changes in irrigation infrastructure from changing water resources and food demand.

We address both of these short-comings. First, we provide supply curves to expand irrigated land at a disaggregated, water region level in addition to the aggregated IRU level for use in the EPPA model. While these supply curves include underlying assumptions on a constant climate, crop mix, and economic environment, this work paves the way for future study in representing irrigable land expansion under alternative assumptions. Second, we provide estimates of current irrigated and rainfed production value at a finer spatial resolution, as well as aggregated to the GTAP 9 regions and crop sectors. We also compute a relative error value for specific GTAP regions and crops to guide researchers and AGE modelers in adjusting production value estimates based on output shares. This work incorporates a global dataset of both documented and estimated crop prices that in future work deserves a more nuanced approach to its development. Finally, we make available the complete set of data and code needed to aggregate the 126 water-region irrigable land supply curves, to directly quantify the current production value of irrigated land, and to evaluate differences in the validity of estimating production values based on output volumes. We hope this access will provide useful data and tools for the integrated assessment community and for those working on natural resource links in economy-wide models.

Acknowledgments

The authors acknowledge support for this work from U.S. Department of Energy, Office of Science (DE-FG02-94ER61937) and also acknowledge support for the basic development of the MIT Integrated Assessment Model (IGSM) from the Joint Program on the Science and Policy of Global Change, which is funded by a consortium of industrial sponsors and federal grants. For a complete list of sponsors see http://globalchange.mit.edu/sponsors/current.html. The findings in this study are solely the opinions of the authors.

References

Aguiar, A., B. Narayanan, and R. McDougall. 2016. "An Overview of the GTAP 9 Data Base." *Journal of Global Economic Analysis*, 1(1). doi:10.21642/JGEA.010103AF.

Beringer, T., W. Lucht, and S. Schaphoff. 2011. "Bioenergy production potential of global biomass plantations under environmental and agricultural constraints." *GCB Bioenergy*, 3: 299-312. doi:10.1111/j.1757-1707.2010.01088.x.

Bonan, G.B., K.W. Oleson, M. Vertenstein, S. Lewis, X. Zeng, Y. Dai, R.E. Dickinson, and Yang, Z.-L. 2002. "The Land Surface Climatology of the Community Land Model Coupled to the NCAR Community Climate Model." *Journal of Climate*, 15: 3123–3149. doi:10.1175/1520-0442(2002)015%3C3123:TLSCOT%3E2.0.CO;2.

Calvin, K., M. Wise, P. Kyle, P. Patel, L. Clarke, and J. Edmonds. 2014. "Trade-offs of different land and bioenergy policies on the path to achieving climate targets." *Climatic Change*, 123(3-4): 691-704. doi:10.1007/s10584-013-0897-y.

Chen, Y.-H.H., S. Paltsev, J. Reilly, J. Morris, V. Karplus, A. Gurgel, N. Winchester, P. Kishimoto, É. Blanc, and M. Babiker. 2017. "The MIT Economic Projection and Policy Analysis (EPPA) Model: Version 5." Technical Note No. 16, MIT Joint Program on the Science and Policy of Global Change. http://globalchange.mit.edu/publication/16620.

Fant, C., A. Gueneau, K. Strzepek, S. Awadalla, W. Farmer, É. Blanc, and C.A. Schlosser. 2012. "CliCrop: a Crop Water-Stress and Irrigation Demand Model for an Integrated Global Assessment Modeling Approach." Working Paper No. 214, MIT Joint Program on the Science and Policy of Global Change. http://globalchange.mit.edu/publication/15732.

Fipps, Guy. 2000. "Characterization of Conveyance Losses in Irrigation Distribution Networks in the Lower Rio Grande Valley of Texas." Texas Water Resources Institute. Texas A&M University. http://idea.tamu.edu/documents/report10.pdf.

Food and Agriculture Organization of the United Nations (FAO). 1989. Irrigation Water Management: Irrigation Scheduling. Rome, Italy. http://www.fao.org/docrep/T7202E/t7202e00.htm#Contents.

Food and Agriculture Organization of the United Nations (FAO). 2015a. Crops. FAOSTAT. Rome, Italy. http://www.fao.org/faostat/en/#data/QC.

Food and Agriculture Organization of the United Nations (FAO). 2015b. AQUASTAT. Rome, Italy. http://www.fao.org/nr/water/aquastat/main/index.stm.

Food and Agriculture Organization of the United Nations (FAO). 2015c. Producer Prices - Annual. FAOSTAT. Rome, Italy. http://www.fao.org/faostat/en/#data/PP.

Gillingham, K.T., S.J. Smith, and R.D. Sands. 2008. "Impact of bioenergy crops in a carbon dioxide constrained world: an application of the MiniCAM energy-agriculture and land use model." Mitigation and Adaptation Strategies for Global Change, 13(7): 675-701. doi:10.1007/s11027-007-9122-5.

Haqiqi, I., F. Taheripour, J. Liu, and D. van der Mensbrugghe. 2016. "Introducing Irrigation Water into GTAP Data Base Version 9." *Journal of Global Economic Analysis*, 1(2). doi:10.21642/JGEA.010203AF.

Johansson, D.J.A. and C. Azar. 2007. "A scenario based analysis of land competition between food and bioenergy production in the US." *Climatic Change*, 82(3–4): 267–291. doi:10.1007/s10584-006-9208-1.

Liu, J., T. Hertel, and F. Taheripour. 2016. "Analyzing Future Water Scarcity in Computable General Equilibrium Models." *Water Economics and Policy*, 2(4). doi:10.1142/S2382624X16500065.

Liu, J., T. Hertel, F. Taheripour, T. Zhu, and C. Ringler. 2014. "International trade buffers the impact of future irrigation shortfalls." *Global Environmental Change*, 29: 22–31. doi:10.1016/j.gloenvcha.2014.07.010.

Natural Resources Conservation Service (NRCS). 2014. Annual and Perennial Crop List. United States Department of Agriculture. Washington, D.C., United States.

Peters, J.C. 2016. "The GTAP-Power Data Base: Disaggregating the Electricity Sector in the GTAP Data Base." *Journal of Global Economic Analysis*, 1(1): 209–250. doi:10.21642/JGEA.010104AF.

Popp, J., Z. Lakner, M. Harangi-Rákos, and M. Fári. 2014. "The effect of bioenergy expansion: Food, energy, and environment." *Renewable and Sustainable Energy Reviews*, 32: 559-578. doi:10.1016/j.rser.2014.01.056.

Portmann, F.T., S. Siebert, and P. Döll. 2010. "MIRCA2000-Global monthly irrigated and rainfed crop areas around the year 2000: A new high-resolution data set for agricultural and hydrological modeling." *Global Biogeochemical Cycles*, 24(1). doi:10.1029/2008GB003435.

Reilly, J., J. Melillo, Y. Cai, D. Kicklighter, A. Gurgel, S. Paltsev, T. Cronin, A. Sokolov, and A. Schlosser. 2012. "Using Land to Mitigate Climate Change: Hitting the Target, Recognizing the Trade-offs." *Environmental Science & Technology*, 46(11): 5672-5679. doi:10.1021/es2034729.

Rosegrant, M.W. and the IMPACT Development Team. 2012. "International Model for Policy Analysis of Agricultural Commodities and Trade (IMPACT): Model Description." International Food Policy Research Institute (IFPRI). Washington, D.C., United States. https://www.researchgate.net/publication/275582667_IMPACT_Technical_Description.

Rutherford, T.F. 2002. Lecture notes on constant elasticity functions. University of Colorado. Boulder, United States. http://www.gamsworld.org/mpsge/debreu/ces.pdf.

Siebert, S. and P. Döll. 2010. "Quantifying blue and green virtual water contents in global crop production as well as potential production losses without irrigation." *Journal of Hydrology*, 384(3–4): 198–217. doi:10.1016/j.jhydrol.2009.07.031.

Smyth, B.M., B.P. Ó Gallachóir, N.E. Korres, and J.D. Murphy. 2010. "Can we meet targets for biofuels and renewable energy in transport given the constraints imposed by policy in agriculture and energy?" *Journal of Cleaner Production*, 18(16-17): 1671-1685. doi:10.1016/j.jclepro.2010.06.027.

Sokolov, A.P., C.A. Schlosser, S. Dutkiewicz, S. Paltsev, D.W. Kicklighter, H.D. Jacoby, R.G. Prinn, C.E. Forest, J.M. Reilly, C. Wang, B. Felzer, M.C. Sarofim, J. Scott, P.H. Stone, J.M. Melillo, and J. Cohen. 2005. "The MIT Integrated Global System Model (IGSM) Version 2: Model Description and Baseline Evaluation." Working Paper No. 124, MIT Joint Program on the Science and Policy of Global Change. http://globalchange.mit.edu/publication/14579.

Strzepek, K., A. Schlosser, A. Gueneau, X. Gao, É. Blanc, C. Fant, B. Rasheed, and H.D. Jacoby. 2013. "Modeling water resource systems within the framework of the MIT Integrated Global System Model: IGSM-WRS." *Journal of Advances in Modeling Earth Systems*, 5(3): 638–653. doi:10.1002/jame.20044.

Taheripour, F., T.W. Hertel, and J. Liu. 2013a. "Introducing water by river basin into the GTAP-BIO model: GTAP-BIO-W." GTAP Working Paper No. 77, Center for Global Trade Analysis. https://www.gtap.agecon.purdue.edu/resources/res_display.asp?RecordID=4304.

Taheripour, F., T.W. Hertel, and J. Liu. 2013b. "The role of irrigation in determining the global land use impacts of biofuels." *Energy, Sustainability and Society*, 3:4. doi:10.1186/2192-0567-3-4.

Taheripour, F., T.W. Hertel, B. Narayanan, and S. Sahin. 2016. "Economic and Land Use Impacts of Improving Water Use Efficiency in Irrigation in South Asia." *Journal of Environmental Protection*, 7(11): 1571–1591. doi:10.4236/jep.2016.711130.

Timilsina, G.R., J.C. Beghin, D. van der Mensbrugghe, and S. Mevel. 2012. "The impacts of biofuels targets on land-use change and food supply: A global CGE assessment." Agricultural Economics, 43: 315-332. doi:10.1111/j.1574-0862.2012.00585.x.

Wallace, J.S. 2000. "Increasing agricultural water use efficiency to meet future food production." Agriculture, Ecosystems and Environment, 82: 105-119. doi:10.1016/S0167-8809(00)00220-6.

Wiberg, D. and K.M. Strzepek. 2005. "Development of Regional Economic Supply Curves for Surface Water Resources and Climate Change Assessments: A Case Study of China." IIASA Research Report. IIASA, Laxenburg, Austria: RR-05-001.

Winchester, N., K. Ledvina, K. Strzepek, and J.M. Reilly. 2018. "The Impact of Water Scarcity on Food, Bioenergy and Deforestation." Australian Journal of Agricultural and Resource Economics, in press.

Winchester, N. and J.M. Reilly. 2015. The feasibility, costs, and environmental implications of large-scale biomass energy. *Energy Economics*, 51: 188–203. doi:10.1016/j.eneco.2015.06.016.

Wise, M., J. Dooley, P. Luckow, K. Calvin, and P. Kyle. 2014. "Agriculture, land use, energy and carbon emission impacts of global biofuel mandates to mid-century." *Applied Energy*, 114: 763–773. doi:10.1016/j.apenergy.2013.08.042.

Appendix A

Table A.1. Water regions within each EPPA region and Irrigation Response Unit (IRU)

EPPA Region	Description	IRU-1	IRU-2	IRU-3	IRU-4
AFR	**Africa**	CAF, EAC, HOA, NIG, VOT, ZAM	NAC, NLE, NWA,SAC, SAH	KAL, LCB, LIM, MAD, ORA, SAF, SEN, WAC	CON
ANZ	**Australia-New Zealand**	CAU	EAU, MAU, WAU	NZE	PAO
ASI	**Dynamic Asia**	BOR, INW, MEK, PHI, TMM	SKP	INE	--
BRA	**Brazil**	NEB	AMA, TOC	SAN	--
CAN	**Canada**	CAN	CCA, GLA	RWI	--
CHN	**China**	LAJ, LMO, SEA	HAI, HUL, HUN, SON, YHE	CHJ, ZHJ	--
EUR	**European Union**	ELB, SCA	BRI, RHI	IEM, IRE, IWA, SEO	ITA, LBO, RHO
IND	**India**	BRR, GAN, GOD, KRI, LUN, MAT	CAV, CHO, EGH, IEC, SAY	--	--
JPN	**Japan**	JAP	--	--	--
LAM	**Other Latin America**	CHC, ORI, RIC	CAM, CAR, CUB, NSA	NSA, PAR, PEC, SAL, TIE, URU	--
MES	**Middle East**	EME, WAI	ARA, TIG	--	--
MEX	**Mexico**	UME, YUC	MIM	--	--
REA	**Rest of East Asia**	NKP, ROW	BRT, IND, SRL	--	--
ROE	**Rest of Europe and Central Asia**	AMD, DAN	SYD	BAL, BLA, DNI, LBA, ODE	--
RUS	**Russia**	OB	AMR, NER, VOG, YEN	UMO, URA	--
USA	**United States**	ARK, MIS, MOU	COB, GBA, SEU	CAL, COL, USN	OHI, RIG, WGM

Source: Mapping defined by authors.

Appendix B

Table B.1. Mapping of FAO crops to MIRCA2000 crops

MIRCA2000 Crop	FAO Crop				
Barley	Barley				
Cassava	Cassava				
Citrus	Fruit, citrus nes	Grapefruit (inc. pomelos)	Lemons and limes	Oranges	Tangerines, mandarins, clementines, satsumas
Cocoa	Cocoa, beans				
Coffee	Coffee, green				
Cotton	Cotton lint				
Date palm	Dates				
Fodder	Maize	Rye	Wheat		
Grapes/vine	Grapes				
Groundnuts/ peanuts	Groundnuts, with shell				
Maize	Maize				
Millet	Millet				
Oil palm	Oil, palm fruit				
Others Annual	Anise, badian, fennel, coriander Beans, green Buckwheat Cabbages and other brassicas Canary seed Carrots and turnips Cauliflowers and broccoli Cereals, nes Chillies and peppers, dry	Chillies and peppers, green Cucumbers and gherkins Eggplants (aubergines) Fibre crops nes Flax fibre and tow Fonio Garlic Ginger Grain, mixed Hemp tow waste Hempseed Jute	Leeks, other alliaceous vegetables Lettuce and chicory Linseed Lupins Melons, other (inc.cantaloupes) Melonseed Mushrooms and truffles Mustard seed Oats Oil, stillingia Oilseeds nes	Okra Onions, dry Onions, shallots, green Peas, green Pineapples Popcorn Poppy seed Pumpkins, squash and gourds Quinoa Roots and tubers, nes Safflower seed	Sesame seed Spinach Strawberries String beans Sugar crops, nes Sweet potatoes Taro (cocoyam) Tobacco, unmanufactured Tomatoes Triticale Vegetables, fresh nes Watermelons Yams Yautia (cocoyam)

Continued

Table B.1. Mapping of FAO crops to MIRCA2000 crops (continued)

MIRCA2000 Crop	FAO Crop				
Others perennial	Agave fibres nes Almonds, with shell Apples Apricots Areca nuts Artichokes Asparagus Avocados Bananas Berries nes Blueberries Brazil nuts, with shell Carobs Cashew nuts, with shell	Cashewapple Castor oil seed Cherries Cherries, sour Chestnut Chicory roots Cinnamon (canella) Cloves Cocoa, beans Coconuts Cranberries Currants Dates Figs Fruit, fresh nes	Gooseberries Gums, natural Hazelnuts, with shell Hops Jojoba seed Kapok fruit Karite nuts (sheanuts) Kiwi fruit Kola nuts Mangoes, mangosteens, guavas Manila fibre (abaca)	Maté Plantains Plums and sloes Nutmeg, mace and cardamoms Nuts, nes Olives Papayas Peaches and nectarines Pears Pepper (piper spp Peppermint Persimmons	Pistachios Pyrethrum, dried Quinces Ramie Raspberries Rubber, natural Sisal Spices, nes Tallowtree seed Tea Tea nes Tung nuts Vanilla Walnuts, with shell
Potatoes	Potatoes				
Pulses	Bambara beans Beans, dry	Broad beans, horse beans, dry	Chick peas Cow peas, dry Lentils	Lupins Peas, dry	Pigeon peas Pulses, nes Vetches
Rapeseed/ canola	Rapeseed				
Rice	Rice, paddy				
Rye	Rye				
Sorghum	Sorghum				
Soybeans	Soybeans				
Sugar beet	Sugar beet				
Sugarcane	Sugar cane				
Sunflower	Sunflower seed				
Wheat	Wheat				

Source: Mapping defined by authors. MIRCA2000 crops are from Portmann et al. 2010. FAO crops are from FAO (2015c).

Table B.2. Pairings of countries missing prices and countries providing proxy prices

Country Missing Prices	Country Providing Proxy Prices	Country Missing Prices	Country Providing Proxy Prices
Afghanistan	Pakistan	Mauritania	Mali
Angola	Namibia	Montenegro	Bosnia and Herzegovina
Benin	Togo	Myanmar	Thailand
Central African Republic	Cameroon	North Korea	South Korea
Chad	Niger	Oman	Yemen
Cuba	Dominican Republic	Papua New Guinea	Indonesia
Democratic Republic of the Congo	Congo	Sierra Leon	Guinea
Djibouti	Eritrea	Somalia	Ethiopia
Gabon	Cameroon	South Sudan	Sudan
Haiti	Dominican Republic	Swaziland	South Africa
Iraq	Iran	Syria	Lebanon
Kuwait	Qatar	Uganda	Rwanda
Lesotho	South Africa	United Arab Emirates	Qatar
Liberia	Ivory Coast	Uzbekistan	Kazakhstan
Libya	Algeria	Zambia	Botswana
Liechtenstein	Switzerland	Zimbabwe	Botswana

Source: Pairings defined by authors.

Appendix C

We compare production value shares calculated (1) by multiplying output volumes by prices and (2) by assuming that production value shares are equal to output volume shares, as in Haqiqi et al. (2016). **Table C.1** summarizes global production values calculated under the two methods. To compare the two value estimates for each crop sector, we compute a "value ratio" defined as the irrigated production value estimated from output share divided by the irrigated production value calculated using our price dataset, and present the average value ratio across GTAP regions. Deviations from a value ratio of 1.0 in the homogenous crop sectors can be attributed to shapefile variations in the price and production datasets.

Table C.1. Irrigated crop production values under alternative methods

Crop Sector	(1) From Output Share		(2) Direct Calculation		Average Ratio of Values (1)/(2)
	Irrigated Value (Million USD)	*Irrigated Value Share*	*Irrigated Value (Million USD)*	*Irrigated Value Share*	
Vegetables and fruit (v-f)	42,355	32.0%	40,164	30.4%	1.09
Coarse grains (gro)	37,504	30.2%	38,119	30.7%	1.02
Other crops (ocr)	130,319	22.8%	147,801	25.8%	1.02
Wheat (wht)	30,908	43.9%	30,915	43.9%	1.01
Sugar crops (c-b)	16,334	52.2%	16,336	52.2%	1.00
Paddy rice (pdr)	95,626	81.0%	95,613	81.0%	0.99
Plant-based fiber (pfb)	52,878	69.6%	52,904	69.7%	0.98
Oilseeds (osd)	6,887	11.4%	7,707	12.8%	0.95
All crops	**412,811**	**34.8%**	**429,559**	**36.3%**	**1.01**

Source: Authors' calculations.

We compare production value estimates by GTAP region and crop sector to flag cases where the two methods yield significantly different results. While we expect comparable estimates within homogeneous crop sectors — wheat (wht), paddy rice (pdr), and plant-based fiber (pbf) — we note that in addition to the v-f sector highlighted in the main text, the heterogeneous oilseed (osd) and other crop (ocr) sectors also yield different irrigated crop value shares for certain GTAP regions (see **Figures C.1 and C.2**).

Interestingly, the two methods actually produce comparable estimates within the sugar crop sector (c-b) even though the c-b sector contains two crops, sugarcane and sugar beet. Labeled in **Figure C.3,** Venezuela and India are among the countries with greater than 75% irrigated sugar crop production. In Venezuela, both sugarcane and sugar beet sell for about $223/t, so the crops' irrigated output shares are approximately equal to their irrigated value shares. In India, nearly all of the c-b production is sugarcane rather than sugar beet, so sugarcane's

contributions to rainfed and irrigated c-b production approach 100% while sugar beet's contributions to irrigated and rainfed production approach 0%. A heavy focus on one sugar crop or the other is characteristic of many of the GTAP regions, and therefore the output share often provides a reasonable estimate for value share. The region XSA – consisting of Afghanistan, Bhutan, and Maldives – is an exception to this trend, however, because both sugarcane and sugar beet are produced, and the price per tonne of sugar beet is exceptionally high relative to the price per tonne of sugar cane. Specifically, the price ratio of sugar beet to sugar cane is 2.74 times higher in XSA than in the average region producing both crops.

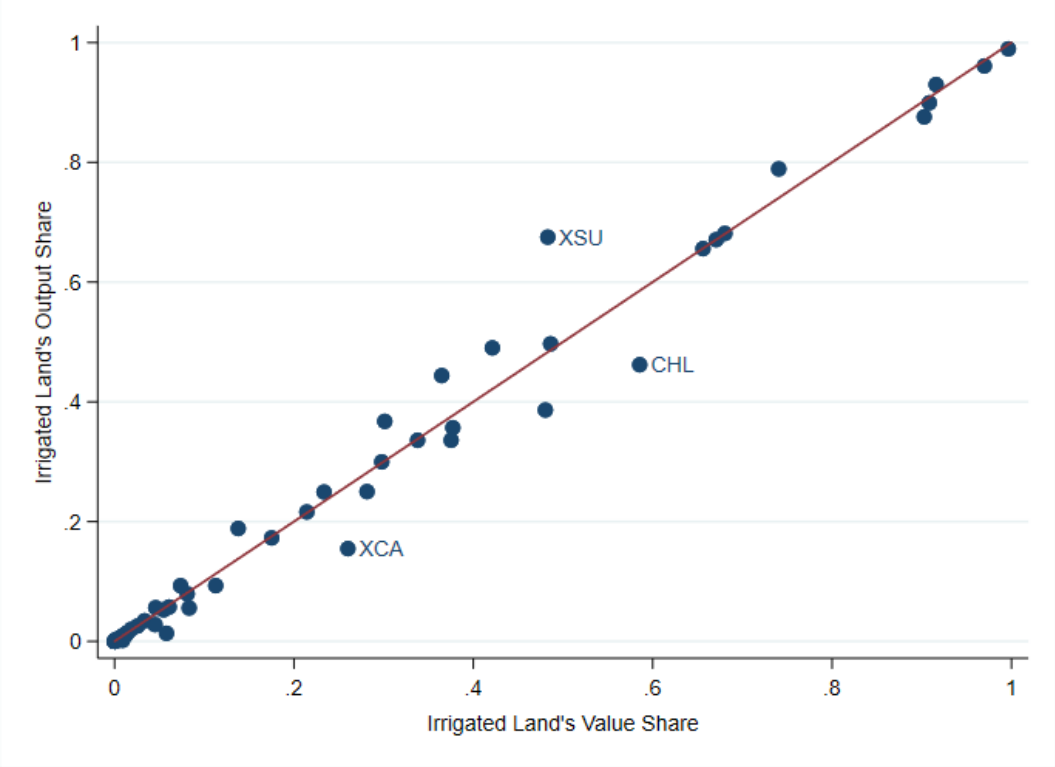

Figure C.1. Irrigated share of production value estimated from the output share (y-axis) versus direct calculation (x-axis) for the **oilseed (osd) sector**.

Notes: Points represent GTAP regions. The red line marks 45 degrees.

Source: Authors' calculation using Portmann et al. (2010), Siebert and Döll (2010), and FAO (2015a, 2015c). Crop mapping from Haqiqi et al. (2016).

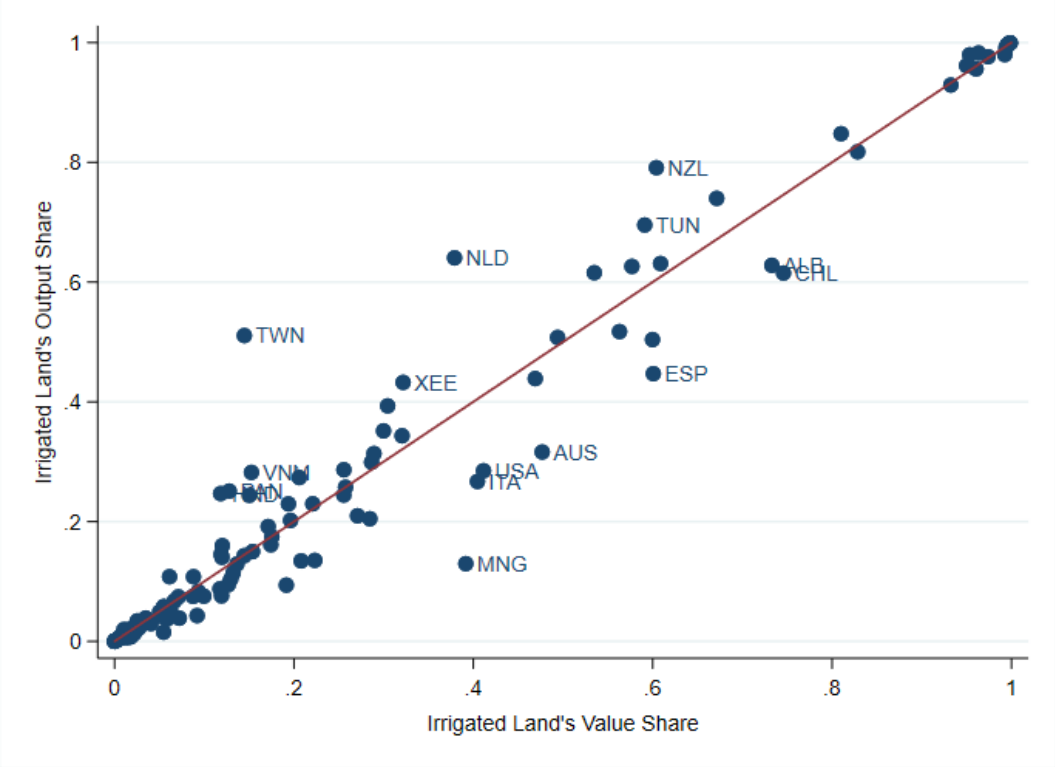

Figure C.2. Irrigated share of production value estimated from the output share (y-axis) versus direct calculation (x-axis) for the **other crop (ocr) sector**.

Notes: Points represent GTAP regions. The red line marks 45 degrees.

Source: Authors' calculation using Portmann et al. (2010), Siebert and Döll (2010), and FAO (2015a, 2015c). Crop mapping from Haqiqi et al. (2016).

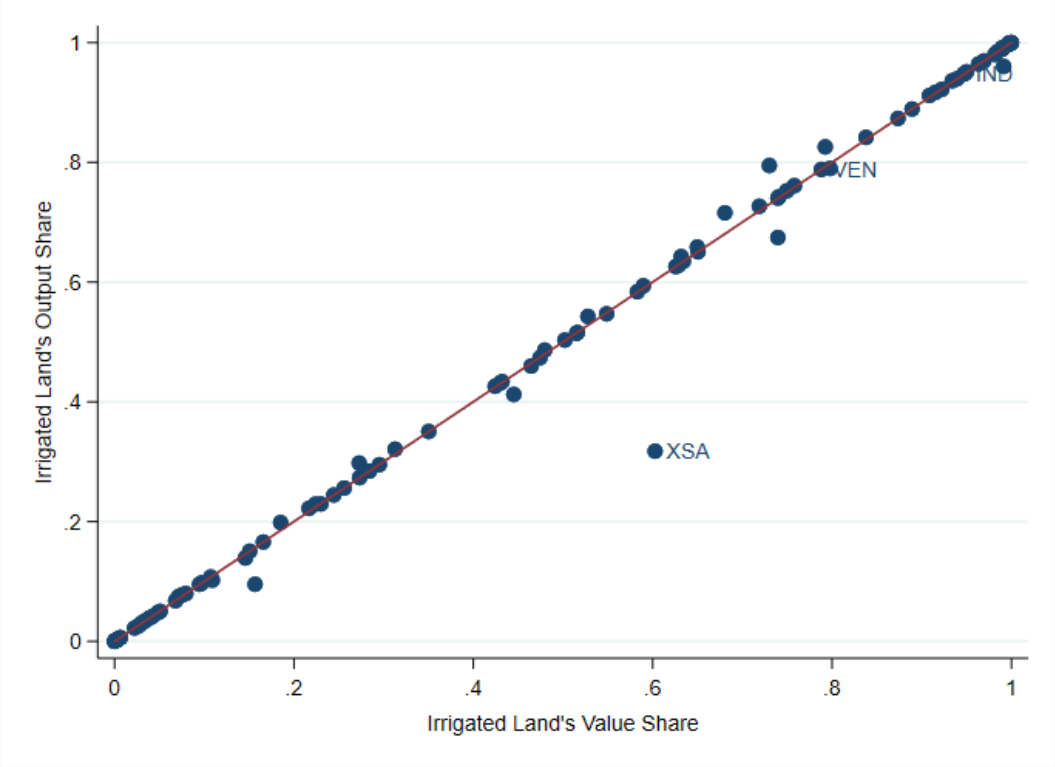

Figure C.3. Irrigated share of production value estimated from the output share (y-axis) versus direct calculation (x-axis) for the **sugar crop (c-b) sector**.

Notes: Points represent GTAP regions. The red line marks 45 degrees.

Source: Authors' calculation using Portmann et al. (2010), Siebert and Döll (2010), and FAO (2015a, 2015c). Crop mapping from Haqiqi et al. (2016).

Joint Program Reprint Series - Recent Articles

For limited quantities, Joint Program publications are available free of charge. Contact the Joint Program office to order.
Complete list: http://globalchange.mit.edu/publications

2018-8 New data for representing irrigated agriculture in economy-wide models. Ledvina, K., N. Winchester, K. Strzepek and J.M. Reilly, *Journal of Global Economic Analysis* 3(1): 122–155 (2018)

2018-7 Sectoral aggregation error in the accounting of energy and emissions embodied in trade and consumption. Zhang, D., J. Caron and N. Winchester, *Journal of Industrial Ecology*, online first (doi: 10.1111/jiec.12734) (2018)

2018-6 Potential Impacts of Climate Warming and Changing Hot Days on the Electric Grid: A Case Study for a Large Power Transformer (LPT) in the Northeast United States. Gao, X., C.A. Schlosser and E. Morgan, *Climatic Change* 147(1-2): 107–118 (2018)

2018-5 Toward a consistent modeling framework to assess multi-sectoral climate impacts. Monier, E., S. Paltsev, A. Sokolov, Y.-H.H. Chen, X. Gao, Q. Ejaz, E. Couzo, C. Schlosser, S. Dutkiewicz, C. Fant, J. Scott, D. Kicklighter, J. Morris, H. Jacoby, R. Prinn and M. Haigh, *Nature Communications* 9: 660 (2018)

2018-4 Tight Oil Market Dynamics: Benchmarks, Breakeven Points, and Inelasticities. Kleinberg, R.L., S. Paltsev, C.K.E. Ebinger, D.A. Hobbs and T. Boersma, *Energy Economics* 70: 70–83 (2018)

2018-3 The Impact of Water Scarcity on Food, Bioenergy and Deforestation. Winchester, N., K. Ledvina, K. Strzepek and J.M. Reilly, *Australian Journal of Agricultural and Resource Economics*, online first (doi:10.1111/1467-8489.12257) (2018)

2018-2 Modelling Ocean Colour Derived Chlorophyll-a. Dutkiewicz, S., A.E. Hickman and O. Jahn, *Biogeosciences* 15: 613–630 (2018)

2018-1 Hedging Strategies: Electricity Investment Decisions under Policy Uncertainty. Morris, J., V. Srikrishnan, M. Webster and J. Reilly, *Energy Journal*, 39(1) (2018)

2017-24 Towards a Political Economy Framework for Wind Power: Does China Break the Mould?. Karplus, V.J., M. Davidson and F. Kahrl, Chapter 13 in: *The Political Economy of Clean Energy Transitions*, D. Arent, C. Arent, M. Miller, F. Tarp, O. Zinaman (eds.), UNU-WIDER/Oxford University Press, Helsinki, Finland (2017)

2017-23 Carbon Pricing under Political Constraints: Insights for Accelerating Clean Energy Transitions. Karplus, V.J. and J. Jenkins, Chapter 3 in: *The Political Economy of Clean Energy Transitions*, D. Arent, C. Arent, M. Miller, F. Tarp, O. Zinaman (eds.), UNU-WIDER/Oxford University Press, Helsinki, Finland (2017)

2017-22 "Climate response functions" for the Arctic Ocean: a proposed coordinated modelling experiment. Marshall, J., J. Scott and A. Proshutinsky, *Geoscientific Model Development* 10: 2833–2848 (2017)

2017-21 Aggregation of gridded emulated rainfed crop yield projections at the national or regional level. Blanc, É., *Journal of Global Economic Analysis* 2(2): 112–127 (2017)

2017-20 Historical greenhouse gas concentrations for climate modelling (CMIP6). Meinshausen, M., E. Vogel, A. Nauels, K. Lorbacher, N. Meinshausen, D. Etheridge, P. Fraser, S.A. Montzka, P. Rayner, C. Trudinger, P. Krummel, U. Beyerle, J.G. Cannadell, J.S. Daniel, I. Enting, R.M. Law, S. O'Doherty, R.G. Prinn, S. Reimann, M. Rubino, G.J.M. Velders, M.K. Vollmer, and R. Weiss, *Geoscientific Model Development* 10: 2057–2116 (2017)

2017-19 The Future of Coal in China. Zhang, X., N. Winchester and X. Zhang, *Energy Policy,* 110: 644–652 (2017)

2017-18 Developing a Consistent Database for Regional Geologic CO2 Storage Capacity Worldwide. Kearns, J., G. Teletzke, J. Palmer, H. Thomann, H. Kheshgi, H. Chen, S. Paltsev and H. Herzog, *Energy Procedia*, 114: 4697–4709 (2017)

2017-17 An aerosol activation metamodel of v1.2.0 of the pyrcel cloud parcel model: development and offline assessment for use in an aerosol–climate model. Rothenberg, D. and C. Wang, *Geoscientific Model Development,* 10: 1817–1833 (2017)

2017-16 Role of atmospheric oxidation in recent methane growth. Rigby, M., S.A. Montzka, R.G. Prinn, J.W.C. White, D. Young, S. O'Doherty, M. Lunt, A.L. Ganesan, A. Manning, P. Simmonds, P.K. Salameh, C.M. Harth, J. Mühle, R.F. Weiss, P.J. Fraser, L.P. Steele, P.B. Krummel, A. McCulloch and S. Park, *Proceedings of the National Academy of Sciences,* 114(21): 5373–5377 (2017)

2017-15 A revival of Indian summer monsoon rainfall since 2002. Jin, Q. and C. Wang, *Nature Climate Change,* 7: 587–594 (2017)

2017-14 A Review of and Perspectives on Global Change Modeling for Northern Eurasia. Monier, E., D. Kicklighter, A. Sokolov, Q. Zhuang, I. Sokolik, R. Lawford, M. Kappas, S. Paltsev and P. Groisman, *Environmental Research Letters*, 12(8): 083001 (2017)

2017-13 Is Current Irrigation Sustainable in the United States? An Integrated Assessment of Climate Change Impact on Water Resources and Irrigated Crop Yields. Blanc, É., J. Caron, C. Fant and E. Monier, *Earth's Future*, 5(8): 877–892 (2017)

2017-12 Assessing climate change impacts, benefits of mitigation, and uncertainties on major global forest regions under multiple socioeconomic and emissions scenarios. Kim, J.B., E. Monier, B. Sohngen, G.S. Pitts, R. Drapek, J. McFarland, S. Ohrel and J. Cole, *Environmental Research Letters*, 12(4): 045001 (2017)

2017-11 Climate model uncertainty in impact assessments for agriculture: A multi-ensemble case study on maize in sub-Saharan Africa. Dale, A., C. Fant, K. Strzepek, M. Lickley and S. Solomon, *Earth's Future* 5(3): 337–353 (2017)

MIT Joint Program on the Science and Policy of Global Change

Massachusetts Institute of Technology
77 Massachusetts Ave., E19-411
Cambridge MA 02139-4307 (USA)

T (617) 253-7492 F (617) 253-9845
globalchange@mit.edu
http://globalchange.mit.edu